Contribution of Landsat 8 data for the estimation of land surface temperature in Batna city, Eastern Algeria

Article *in* Geocarto International · March 2016

DOI: 10.1080/10106049.2016.1156167

CITATIONS
32

READS
1,426

3 authors, including:

Abdelhalim Bendib
Faculté des sciences de la terre et de l'univers
21 PUBLICATIONS **56** CITATIONS
SEE PROFILE

Dridi Hadda
Universite Batna2 Algerie
22 PUBLICATIONS **100** CITATIONS
SEE PROFILE

Geocarto International

ISSN: 1010-6049 (Print) 1752-0762 (Online) Journal homepage: http://www.tandfonline.com/loi/tgei20

Contribution of Landsat 8 data for the estimation of land surface temperature in Batna city, Eastern Algeria

Abdelhalim Bendib, Hadda Dridi & Mohamed Issam Kalla

To cite this article: Abdelhalim Bendib, Hadda Dridi & Mohamed Issam Kalla (2016): Contribution of Landsat 8 data for the estimation of land surface temperature in Batna city, Eastern Algeria, Geocarto International, DOI: 10.1080/10106049.2016.1156167

To link to this article: http://dx.doi.org/10.1080/10106049.2016.1156167

GEOCARTO INTERNATIONAL, 2016
http://dx.doi.org/10.1080/10106049.2016.1156167

Taylor & Francis
Taylor & Francis Group

Contribution of Landsat 8 data for the estimation of land surface temperature in Batna city, Eastern Algeria

Abdelhalim Bendib, Hadda Dridi and Mohamed Issam Kalla

Laboratory of Natural Hazards and Spatial Planning LRNAT, University of Batna, Batna, Algeria

ABSTRACT

In this study, we presented a mono-window (MW) algorithm for land surface temperature retrieval from Landsat 8 TIRS. MW needs spectral radiance and emissivity of thermal infrared bands as input for deriving LST. The spectral radiance was estimated using band 10, and the surface emissivity value was derived with the help of NDVI and vegetation proportion parameters for which OLI bands 5 and 4 were used. The results in comparison with MODIS (MOD11A1) products indicated that the proposed algorithm is capable of retrieving accurate LST values, with a correlation coefficient of 0.850. The industrial area, public facilities and military area show higher surface temperature (more than 37 °C) in comparison with adjoining areas, while the green spaces in urban areas (34 °C) and forests (29 °C) were the cooler part of the city. These successful results obtained in the study could be used as an efficient method for the environmental impact assessment.

ARTICLE HISTORY
Received 3 December 2015
Accepted 15 February 2016

KEYWORDS
Land surface temperature; Landsat 8 TIRS; MODIS; mono-window algorithm; thermal infrared

1. Introduction

Land surface temperature (LST) is one of the most important parameters in the surface process of land–air interaction (Cristobal et al. 2008; Kuenzer & Dech 2013; Li et al. 2013). Knowledge of the distribution of LST can provide useful information about the surface physical properties and climate which plays a role in a variety of fields including evapotranspiration, climate change, hydrological cycle, vegetation monitoring, urban climate (especially, urban heat island [UHI] effect) and environmental studies. Furthermore, due to the variable changes of LST, the traditional method to measure surface temperature by a thermometer cannot practically obtain large-scale and continuous LST information (Yang et al. 2014). So, development in remote sensing technology and acquired data is recognized as the only viable means to get the LST distribution over the entire globe with sufficient resolution. Today, data from earth observation systems are available and present an opportunity to collect information relevant to urban and peri-urban environments at various spatial, temporal and spectral scales.

Nowadays, in an era of significant technological progress in data, technologies and theories, the above questions still remain important. We need to understand a variety of phenomena, such as urban current temperature changes, urban microclimate dynamics, industry-related thermal water pollution, forest fires flare up and more recently UHI. Temperature is one of the most important physical–environmental variables monitored by Earth-observing remote sensing systems (Worner 2013). Temperature information with good spatial and temporal coverage is a key to addressing most

CONTACT Abdelhalim Bendib halim.bendib@hotmail.com

of these questions and can provide important information about the surface physical properties and climate (Dousset & Gourmelon 2003). The new Landsat Data Continuity Mission, launched on 11 February 2013, with two thermal infrared bands TIR (10 and 11) provided another opportunity. Satellite data and remotely sensed images are useful for the investigation of surface thermal conditions in urban areas (Walawender et al. 2013).

LST is an important parameter for urban climate studies (Heldens et al. 2013). Various studies have been carried out, and different approaches have been proposed to derive LST from satellite TIR data using a variety of methods and algorithms (Qin et al. 2001; Jiménez-Muñoz & Sobrino 2003; Tang et al. 2008; Li et al. 2013). The mono-window (MW) method was first proposed by Qin et al. (2001) to determine the LST from previous Landsat series (such as TM and ETM+). Since then, a variety of improved MW algorithms have been adapted to retrieve LST for Landsat 8 Thermal Infrared Sensor (TIRS) data. In this study, we employed Landsat 8 data and GIS to show how the analysis and spatial distribution of LST for urban area can be carried out based on MW algorithm improved by Wang et al. (2015) using the example of the city of Batna in Eastern Algeria. For the LST retrieval, we firstly present the computation of the brightness temperature. Secondly, we estimate the required parameters (atmospheric transmittance, land surface emissivity and atmospheric water vapour content) for the MW algorithm. Thirdly, we use MODIS LST products to validate our results, and finally, we combine these steps to mapping land surface temperature, with which the urban structure types can be identified.

2. Description of study area

Batna city, the capital of the Aures massif (Figure 1), is located in Eastern Algeria, in the province of Batna, between 35°34′ and 35°31′ North latitude, 6°7′ and 6°13′ East longitude in the middle of a plateau surrounded by mountains having an altitude ranging from 714m to 2192 meters. Batna is characterized by a semi-arid climate; the region has an average annual rainfall of 349.8 mm. The mean monthly air temperature ranges from 4 °C in January to 35 °C in July, with an annual average of 16.7°.

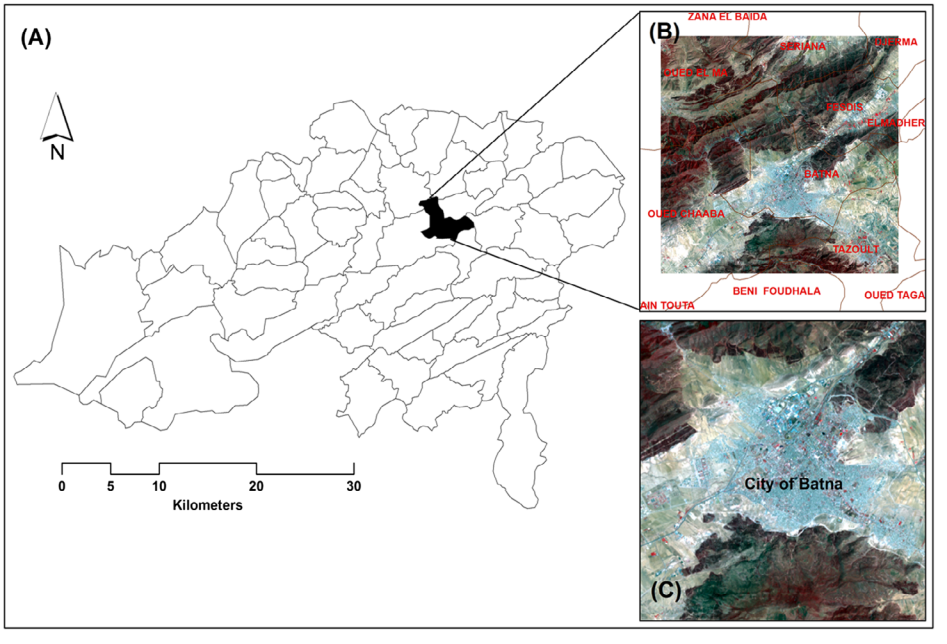

Figure 1. Location of the study area (a) province of Batna (b) city boundary and (c) city of Batna (study area).

Today, the city of Batna is the largest and the main economic centre of the province, where the majority of activities are concentrated in main sectors: the trade (45.50%), the services (38.08%) and industry (16.40%). During the last decade, the territory of the city spreads significantly from 483.43 ha in 1972 to more than 1331.32 ha in 1987 and from 2056.41 ha in 2001 to more than 2852.41 ha in 2013 and the number of registered inhabitants reached 319,742 in 2013. The expansion of the urban area had a remarkable effect on the urban environment; the phenomenon of the UHI effect becomes more and more severe in the city in recent years.

3. Materials and methods

The main goal of this study was therefore to extract changes in LST in the city of Batna. To this end, a remote sensing satellite data from Landsat 8 TIRS were obtained. These satellite data (Table 1) were acquired in the context of work on the characterization of surface temperatures for which summer acquisition date was required to avoid the cloudy pixel problem. For this study, it would have actually been more useful to work on scenes taken in the summer season. Indeed, on the images put in this work, the clouds do not cover our zone of study; however, the images available in the archive acquired in winter and autumn represent important spots of clouds, so we decided to use the present images in order to avoid the effect of clouds, therefore get more representative results. Furthermore, Wang et al. (2015) indicated that data from the Landsat 8 TIRS Band 11 have large uncertainty and suggested using TIRS band 10 data as a single spectral band for LST estimation; for this reason, present work provides the use of L8 band 10.

On the other hand, the information acquired from various satellites data is processed in a multi-software platform, in order to calculate the land surface temperature. For this purpose, we used two complementary software: ArcGis10.1 and ENVI4.7.

This study aimed to test the ability of Landsat thermal sensors to detect the surface temperature of the city of Batna. To achieve this, this study includes the major following steps (Figure 2): conversion of pixel values of the Landsat thermal band to At-sensor spectral radiance, then transformed to at-sensor brightness temperature and LST by adopting MW algorithm.

3.1. TOA spectral radiance

TOA (top of atmospheric) spectral radiance was calculated by multiplying multiplicative radiometric rescaling factor of TIR bands with its corresponding TIR band and adding additive rescaling factor where

$$L\lambda = M_{\mathrm{L}} * Q_{\mathrm{cal}} + A_{\mathrm{L}} \tag{1}$$

where $L\lambda$ is the spectral radiance in watts/(m^{-2} $srad^{-1}$ μm^{-1}); ML is the band-specific multiplicative rescaling factor obtained from the metadata (0.000342); AL is the band-specific additive rescaling factor obtained from the metadata (0.1); Q_{Cal} is the DN value for the quantized and calibrated standard product pixel of band 10.

3.2. Brightness temperature

Brightness temperature is the electromagnetic radiation travelling upward from the top of the Earth's atmosphere (Latif 2014). After getting the radiance value, it should be converted to brightness temperature BT with the help of the following equation:

Table 1. Details of data used in study.

Satellite	Bands	Resolution	Path/Row	Date
Landsat 8 TIRS	10, 5, 4	100 m	194–35	11/6/2015
MODIS (MOD11A1)	31, 32	1 Km	15–8	11/6/2015

$$T_{10} = \frac{K_2}{\mathrm{Ln}\left[\left(\frac{K_1}{K_\lambda}\right) + 1\right]} \tag{2}$$

where T_{10} is the brightness temperature; $K1$ and $K2$ are thermal conversion constants (Table 2), which can be found in the metadata file of the Landsat image; $L\lambda$ is top of atmospheric radiance.

3.3. Land surface emissivity

The emissivity is radiative properties of objects. It characterizes the ability of a body to emit radiation (Rhinane et al. 2012). The knowledge of land surface emissivity is necessary to obtain surface temperature. To do this, Zheng et al. (2010) put forward a set of formula to estimate the emissivity of town and natural surface.

$$\varepsilon_{\text{town}} = 0.9608420 + 0.0860322Pv - 0.0671580Pv^2 \tag{3}$$

$$\varepsilon_{\text{natural}} = 0.9643744 + 0.0614704Pv - 0.0461286Pv^2 \tag{4}$$

where Pv represents the vegetation proportion obtained according to (Carlson & Ripley 1997):

$$Pv = \left[\frac{\text{NDVI} - \text{NDVI}_s}{\text{NDVI}_v - \text{NDVI}_s}\right]^2 \tag{5}$$

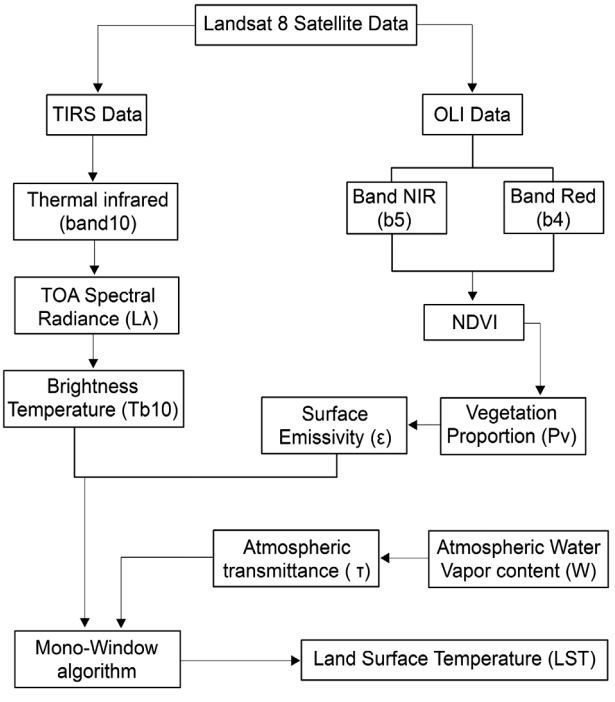

Figure 2. The main flowchart of retrieving LST from Landsat 8 image.

Table 2. K1 and K2 values.

Thermal constant	Band 10	Band 11
K1	777.89	480.89
K2	1321.08	1201.14

NDVI: Normalized difference vegetation index, calculated as the combination of band near infrared and red:

$$\mathrm{NDVI} = \frac{\mathrm{Red} - \mathrm{NIR}}{\mathrm{Red} + \mathrm{NIR}} \tag{6}$$

$\mathrm{NDVI_s}$ (or $\mathrm{NDVI_{min}}$) is the NDVI of soil, in our study area equal to −0.096
$\mathrm{NDVI_v}$ (or $\mathrm{NDVI_{max}}$) is the NDVI of vegetation equal to 0.4

3.4. Land surface temperature

The LST can be obtained by adopting MW algorithm developed by Qin et al. (2001) for Landsat TM6. According to Wang et al. (2015), we adopted the MW algorithm in the following form for LST retrieval from L8 TIRS (B10):

$$T_s = \frac{1}{c_{10}}\{a(1 - C_{10} - D_{10}) + [b(1 - C_{10} - D_{10}) + C_{10} + D_{10}]T_{10} - D_{10}T_a\} \tag{7}$$

where T_s is the LST in Kelvin; T_{10} is the brightness temperature of L8 band 10; T_a is the mean atmospheric temperature; a and b are the constants used to approximate the derivative of the Planck-radiance function for the TIRS band 10 given in Table 3:

C_{10} and D_{10} are the internal parameters for the MW algorithm given as follows:

$$C_{10} = \varepsilon_{10}\tau_{10} \tag{8}$$

$$D_{10} = (1 - \tau_{10})[1 + (1 - \varepsilon_{10})\tau_{10}] \tag{9}$$

$$T_a = 16.0110 + 0.92621T_0 \ (\mathrm{Mid - latitude\ summer}) \tag{10}$$

T_0: The near-surface air temperature.

For estimating the LST by mono-window algorithm, it is necessary to determine the atmospheric transmittance τ and atmospheric water vapour content W. Several authors (Qin et al. 2001; Jiménez-Munoz & Sobrino 2004; Labbi & Mokhnache 2015; Wang et al. 2015) have shown that there is a linear relationship between τ and W in thermal infrared band (Table 4).

The atmospheric content in water vapour can be derived according to the humidity ϕ_r and the partial pressure of water vapour in the air P_s (Rhinane et al. 2012).

$$W = \frac{0.493.\phi_r.P_s}{T} \tag{11}$$

Table 3. Coefficients a and b according to Wang et al. (2015).

Temperature range (°C)	a (band 10)	b (band 10)
20–70	−70.1775	0.4581
0–50	−62.7182	0.4339
−20 to −30	−55.4276	0.4086

Table 4. Estimation of atmospheric transmittance.

Atmospheres	Water Vapour (g cm^{-2})	Transmittance
High air temperature	0.4–1.6	$\tau = 0.974290 - 0.08007w$
	1.6–3.0	$\tau = 1.031412 - 0.11536w$
Low air temperature	0.4–1.6	$\tau = 0.982007 - 0.09611w$
	1.6–3.0	$\tau = 1.053710 - 0.14142w$

$$P_s = e\left[26.23 - \frac{5416}{T}\right] \tag{12}$$

where T is the effective temperature estimated from the air temperature.

4. Results and discussion

Before presenting and discussing the results obtained, current retrieved LST was compared with MODIS derived-LST. Due to the absence of measures on land and synchronized data from the unique local weather station existing, this study aimed to evaluate LST retrieved from Landsat8 TIRS using MODIS LST products as reference.

Moderate Resolution Imaging Spectroradiometer (MODIS) acquires data, which covers the entire earth surface on a near-daily basis in 36 spectral bands that span the visible (0.415 μm) to infrared (14.235 μm) spectra at 1-km, 500-m, and 250-m nadir pixel resolutions. The LST in the MODIS LST product is the radiometric (kinetic) temperature derived from the TIR radiation emitted by the land surface and measured instantaneously by MODIS (Wan & Li 2011).

The images that we have not exactly represent the same standards. The spatial resolution of MODIS products is 1000 m, while the resolution of Landsat8 TIRS is 100 m. Therefore, before integrating the data, a process of resampling the spatial resolution from 1 Km to 100 m was carried out by applying the Pan-Sharpening technique from ENVI4.7 software (Figure 3).

As shown in the following Figure 3, it can be noted that the distribution of the two kinds of LST is overall consistent, but also it can be seen that the values retrieved from MODIS LST are higher than that of Landsat8 TIRS. There is a difference of 4.72 °C (37.91 °C for Landsat and 42.63 °C for MODIS) for the mean values. According to Yang et al. (2014), this may be explained by:

(1) Intervals of 30 min existed between the two sensors as well as rapid changes in LST of impervious surfaces caused by high reflectivity such as town.
(2) The water vapour content parameter required for producing MODIS LST products was retrieved from water vapour absorption property difference between different channels, which has some variance in the water vapour content data obtained by empirical correlation.
(3) In order to make a comparative analysis of the retrieved LST and MODIS LST products, we resampled the spatial resolution of retrieved LST from 1 Km to 100 m; thus, the spatial resolution difference resulted in a scale effect to some extent.

In order to validate the results and analyse the relationship between MODIS LST data and retrieved LST from Landsat8 TIRS, scatter plots and linear fitting were done with the help of 32 samples between

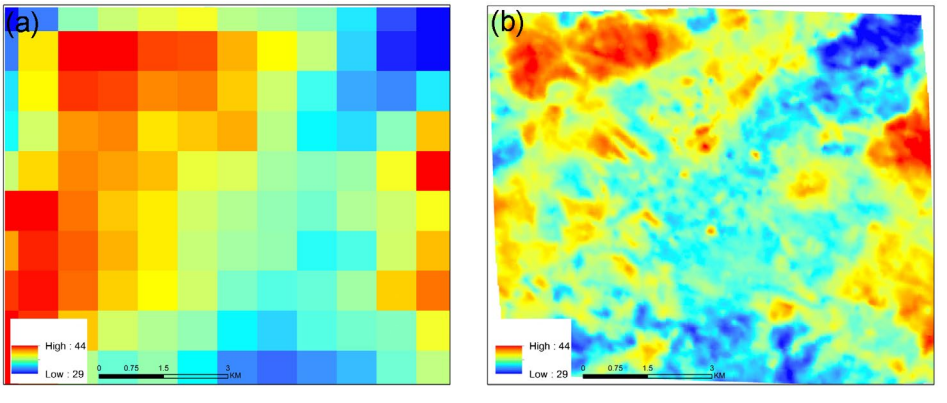

Figure 3. Retrieved LST from MODIS LST (a) and Landsat8 TIRS (b).

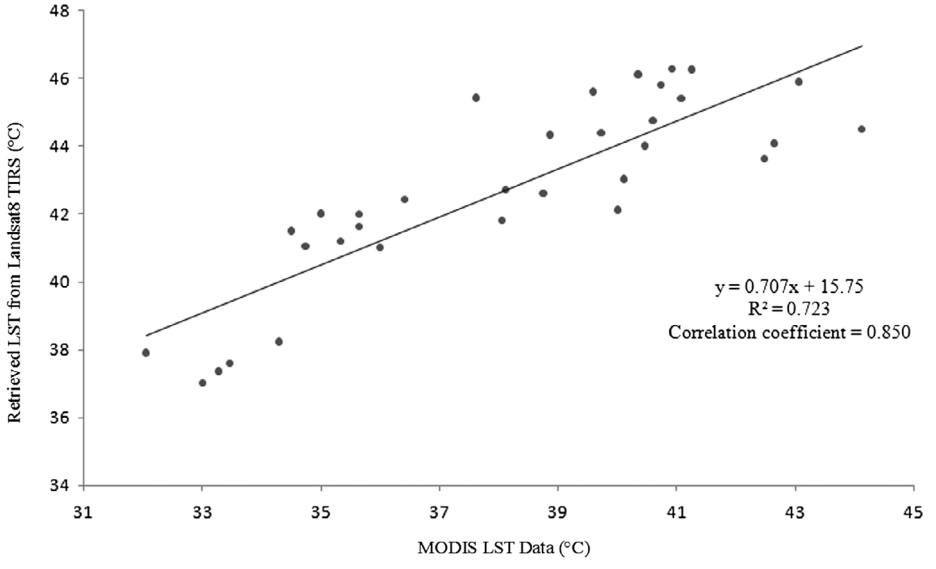

Figure 4. Scatter plots of correlation analyses of retrieved LST and MODIS LST.

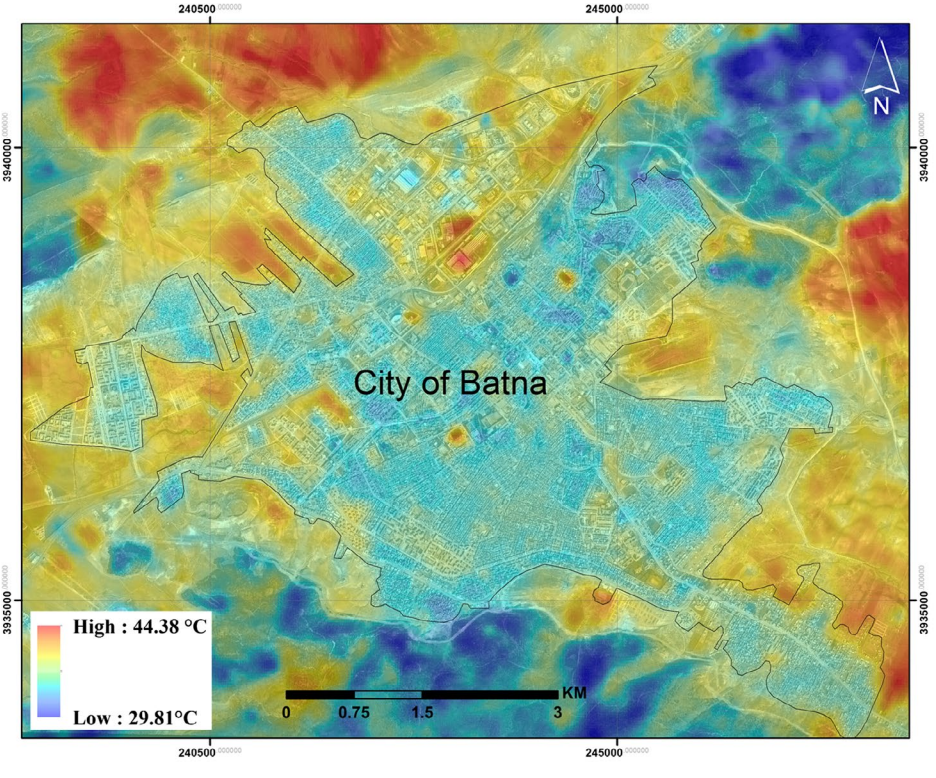

Figure 5. The retrieved LST by MW algorithm of Batna city.

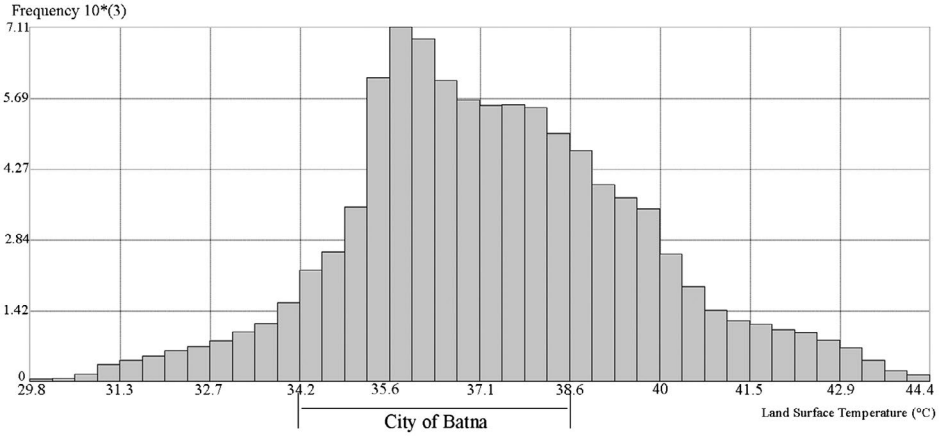

Figure 6. Histogram distribution of LST in the study area.

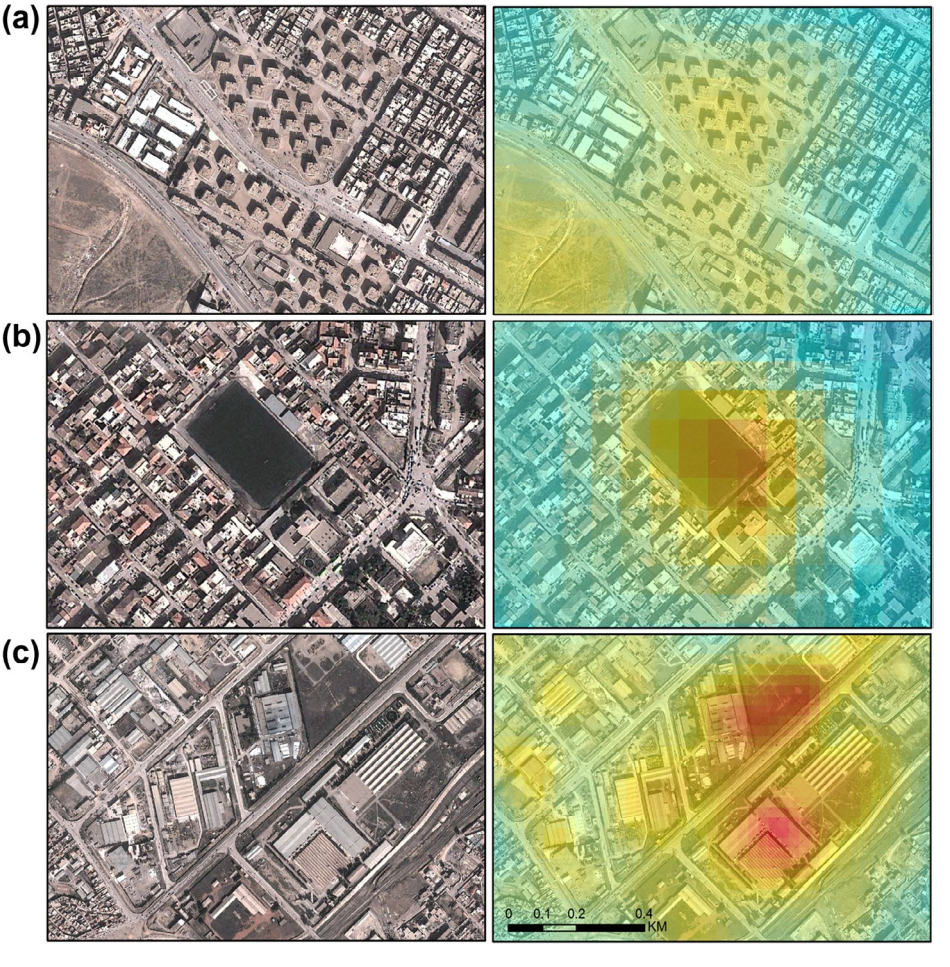

Figure 7. Heat island area (a) social collective habitat, (b) stadium tartan and (c) industrial area.

LST values and the corresponding MODIS values. Statistical analysis showed (Figure 4) that the correlation coefficient reached 0.850, R^2 = 0.723, which means that there was significant positive correlation between LST estimated by MW algorithm and NASA's MODIS data provided by USGS. That is to say, in area with the lack of some parameters to estimate LST, the results obtained have a reliability and accuracy.

The LST of Batna city shown in the following Figure 5 was retrieved from Landsat 8 data using the improved MW algorithm of Wang et al. (2015) according to computed results of surface emissivity and brightness temperature. It can be seen that LST in the study area ranged from 29.81 to 44.38 °C with a mean of 37.91 °C. Statistically, within the study area (8722.54 ha), 35.09% of the surface presents high temperature HT, 53.91% moderate temperature MT and 10.98% low temperature LT. On the whole, the city of Batna was a moderate temperature (Figure 6) since more than 4703 ha of the area falls within the MT categories. Moreover, the figure illustrates that the highest LST was traced in the north, east and west of the study area, where barren lands (1) were mostly found, while the lowest temperatures are marked in the highly elevated regions (2) with dense forests in north-eastern and southern of the study area. Similarly, the moderate temperatures are seen in the urban surface (3).

Three main centres of very high heat emission can be easily distinguished (Figure 7). These are industrial area of the city (43 °C) with total area of 370 ha, social collective habitat (38 °C) and public facilities like stadium tartan (39 °C). Indeed, the strong overheating of these classes is caused by very high heat capacity of predominant artificial surfaces (asphalt, roof sheeting, etc.) but also a very small

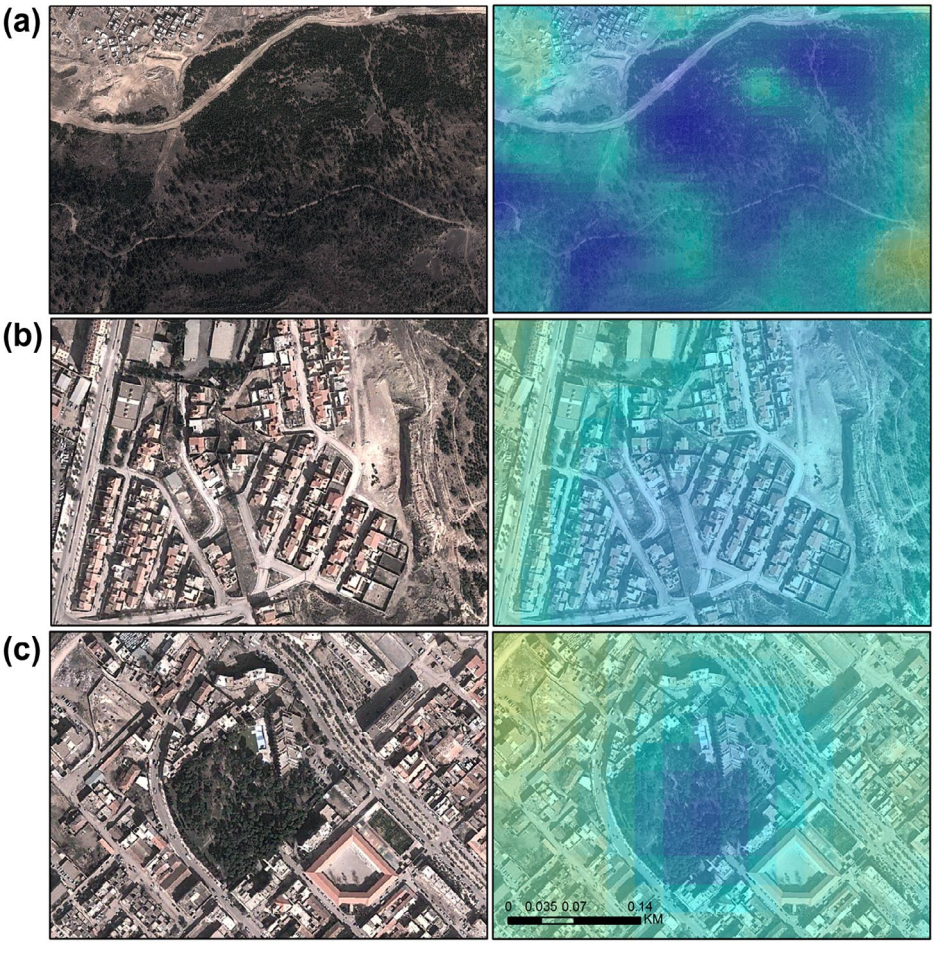

Figure 8. Fresh urban area (a) forests, (b) villa zones and (c) urban greens (park).

share of vegetation between discontinuous urban fabrics. Another feature of LST distribution in the region is that the surrounding bare ground (clay soil and sandstone) has very high LST (more than 40 °C). According to Weng et al. (2004), this is due to the specific thermal properties, such as thermal conductivity, heat capacity and thermal inertia. Additionally, the bare ground surface exposed to solar radiation especially between 08:00 and 12:00 warms up very quickly which makes the contrast between the city and these areas significantly visible (difference of 9 °C). Quantitatively, bare ground occupied 2058.52 ha or 23.60% of the total study area.

On the other hand, the coldest spots in this area are very distinctive. With an area of 1800.26 ha occupied mostly by Aleppo pine (*Pinus halepensis*), the northern slopes covered by the Dj Ich Ali forest (1300 m) and the forest covering southern slopes of Dj Azzeb (1200 m) marked the lowest temperatures (between 31 and 29 °C, respectively). Indeed, as shown in Figure 5, some influence of aspect on the spatial distribution of LST and its relationship with severity levels, cover type and hour of the day is observed. High LST values are systematically registered on SE-facing slopes. Conversely, values corresponding to pixels in NNE- and SW-facing slopes register lower LST.

Temperature reduction by trees is mainly caused by two factors: direct shading and evapotranspirational cooling (Oke 1989). On a hot summer day, lower temperatures are marked also in villa zones (Figure 8(b)) and urban greens with a temperature less than 34 °C. The Figure 8(c) presents one of the biggest and oldest parks in the city of Batna. With a total area of 1.60 ha surrounded by a dense urban fabric, this park clearly shows the climatic impact of green space. LST within this park can be 2–3 °C lower than in the surrounding built-up areas. On the basis of this park, we can conclude that open spaces types with a high percentage cover trees are the most effective vegetation element for reducing overheating in urban areas. This correlation between urban parks and LST is consistent with findings from other published studies (Eliasson 2000; Tyrväinen et al. 2005).

5. Conclusion

In this study, we present a MW algorithm to retrieve LST from Landsat8 TIRS data in the city of Batna. From the results obtained, it is shown that the barren lands (Clay soil and Sandstone) experienced high LST (more than 40 °C). Conversely, Northern and Southern forests occupied by Aleppo pine marked the lowest temperatures (less than 31 °C). Between these two categories, the city of Batna marked moderate values ranged from 35 to 38 °C with some anomalies registered such as industrial area (43 °C) and urban greens (34 °C). With the lack of synchronized measured data, LST products have been validated using *in situ* LST products from MODIS (MOD11A1) data; results of validation and comparison using scatter plots confirm that the correlation coefficient reached 0.850, which demonstrates the applicability of the proposed algorithm in LST retrieval.

The technique presented in this study could be used as an efficient method for the environmental impact assessment. It would be very simple and useful to apply this method to other Algerian cities.

Acknowledgement

The authors are grateful to LRNAT laboratory of Batna University (Algeria), which has provided a platform for this study.

Disclosure statement

No potential conflict of interest was reported by the authors.

References

Carlson TN, Ripley DA. 1997. On the relation between NDVI, fractional vegetation cover, and leaf area index. Remote Sens Environ. 62:241–252.

Cristobal J, Ninyerola M, Pons X. 2008. Modeling air temperature through a combination of remote sensing and GIS data. J Geophys Res. 113:1–13.

Dousset B, Gourmelon F. 2003. Satellite multi-sensor data analysis of urban surface temperatures and landcover. ISPRS J Photogramm Remote Sens. 58:43–54.
Eliasson I. 2000. The use of climate knowledge in urban planning. Landsc Urban Planning. 48:31–44.
Heldens W, Taubenböck H, Esch T, Heiden U, Wurm M. 2013. Analysis of surface thermal patterns in relation to urban structure types: A case study for the city of Munich. In: Kuenzer C, Dech S, editors. Thermal infrared remote sensing: sensors, methods, applications, remote sensing and digital image processing. Heidelberg: Springer Netherlands; p. 475–493.
Jiménez-Muñoz JC, Sobrino JA. 2003. A generalized single-channel method for retrieving land surface temperature from remote sensing data. J Geophys Res. 108:4688–4695.
Jiménez-Munoz JC, Sobrino JA. 2004. Error sources on the land surface temperature retrieved from thermal infrared single channel remote sensing data. Int J Remote Sens. 27:999–1014.
Kuenzer C, Dech S. 2013. Thermal infrared remote sensing: sensors, methods, applications. Remote Sens Digital Image Proces. 17:429–451.
Labbi A, Mokhnache A. 2015. Estimating of total atmospheric water vapor content from MSG1-SEVIRI observations. Atmos Meas Techn Discuss. 8:8903–8923.
Latif MS. 2014. Land Surface temperature retrival of Landsat-8 data using split window algorithm – a case study of Ranchi district. Int J Eng Dev Res (IJEDR). 2:3840–3849.
Li ZL, Tang BH, Wu H, Ren H, Yan G, Wan Z, Trigo IF, Sobrino JA. 2013. Satellite-derived land surface temperature: current status and perspectives. Remote Sens Environ. 131:14–37.
Oke TR. 1989. The micrometeorology of the urban forest. Philos Trans R. Soc B. 324:335–349.
Qin Z, Karnieli A, Berliner P. 2001. A mono-window algorithm for retrieving land surface temperature from Landsat TM data and its application to the Israel-Egypt border region. Int J Remote Sens. 22:3719–3746.
Rhinane H, Hilali A, Bahi H, Berrada A. 2012. Contribution of Landsat data for the detection of urban heat islands areas Case of Casablanca. J Geog Inf Syst. 04:20–26.
Tang BH, Bi Y, Li ZL, Xia J. 2008. Generalized split-window algorithm for estimate of land surface temperature from Chinese geostationary FengYun meteorological satellite (FY-2C) Data. Sensors. 8:933–951.
Tyrväinen L, Pauleit S, Seeland K, Vries S. 2005. Benefits and uses of urban forests and trees. In: Konijnendijk CC, Nilsson K, Randrup ThB, Schipperijn J, editors.Urban forests and trees. Heidelberg: Springer; p. 81–114.
Walawender JP, Szymanowski M, Hajto MJ, Bokwa A. 2013. Land surface temperature patterns in the urban agglomeration of Krakow (Poland) derived from Landsat7 ETM+ data. Pure Appl Geophys. 171:913–940.
Wan Z, Li ZL. 2011. MODIS land surface temperature and emissivity. In: Ramachandran B, Justice CO, Abrams MJ, editors. Land remote sensing and global environmental change NASA's earth observing system and the science of ASTER and MODIS. Heidelberg: Springer-Verlag New York; 567p.
Wang F, Qin Z, Song C, Tu L, Karnieli A, Zhao S. 2015. An improved mono-window algorithm for land surface temperature retrieval from Landsat 8 thermal infrared sensor data. Remote Sens. 7:4268–4289.
Weng Q, Lu D, Schubring J. 2004. Estimation of land surface temperature–vegetation abundance relationship for urban heat island studies. Remote Sens Environ. 89:467–483.
Worner JD. 2013. Thermal infrared remote Sensing sensors, methods, applications. Heidelberg: Springer Netherlands. 17:546p.
Yang L, Cao YG, Zhu XH, Zeng SH, Yang GJ, He JY, Yang WC. 2014. Land surface temperature retrieval for arid regions based on Landsat-8 TIRS data: a case study in Shihezi, Northwest China. J Arid Land. 6:704–716.
Zheng GQ, Lu M, Zhang T. 2010. The impact of difference of land surface emissivity on the land surface temperature retrieval in Jinan City. J Shandong Jianzhu Univ. 25:519–523.